

## Spacetime modulation in floating thin elastic plates

Mohamed Farhat<sup>1,\*</sup>, Sebastien Guenneau<sup>2</sup>, Pai-Yen Chen<sup>3</sup>, and Ying Wu<sup>1,†</sup>

<sup>1</sup>Computer, Electrical, and Mathematical Science and Engineering (CEMSE) Division, King Abdullah University of Science and Technology (KAUST), Thuwal 23955-6900, Saudi Arabia

<sup>2</sup>UMI 2004 Abraham de Moivre-CNRS, Imperial College London, London SW7 2AZ, United Kingdom

<sup>3</sup>Department of Electrical and Computer Engineering, University of Illinois at Chicago, Chicago, Illinois 60607, USA



(Received 15 December 2020; revised 17 June 2021; accepted 21 June 2021; published 29 July 2021)

We consider the propagation of flexural-gravity waves in thin elastic plates floating atop nonviscous fluids, e.g., seawater, which are governed by a partial differential equation with Laplacian and tri-Laplacian terms. We investigate the effect of time modulation as well as spacetime modulation on thin floating elastic plates and show the peculiarity of the phenomena of the  $k$ -band gap and the rotated  $k$ -band gap in the context of flexural-gravity waves. This makes possible floating plates with nonreciprocal features and behaving as elastodynamic analogs of luminal electromagnetic metamaterials, with exotic applications in enhanced control of ocean waves, such as filtering devices, unidirectional acoustic propagation, and isolation effects and energy harvesting in maritime engineering.

DOI: [10.1103/PhysRevB.104.014308](https://doi.org/10.1103/PhysRevB.104.014308)

### I. INTRODUCTION

Metamaterials and metasurfaces consist of a spatially periodic arrangement of meta-atoms in three or two dimensions, respectively [1,2]. These artificial materials were applied successfully in the last two decades to obtain several exciting applications, ranging from superlensing [3] to invisibility cloaks [4], plasmonic waveguides [5], and computing [6]. Such a concept encompasses a broad range of disciplines, including but not limited to acoustic [7], elastic [8], and structural [9] waves, as well as engineering thermal properties [10,11]. All these applications exploited only the space modulation (generally subwavelength). Recently, time also emerged as a promising parameter in designing more appealing metasurfaces. In fact, the place of time in physics is very special. First, this parameter was assumed to be absolute in Newtonian mechanics [12], until Einsteinian mechanics revolutionized its very basic nature and showed that it has to be considered on an equal footing with the remaining spatial variables, i.e., it undergoes changes when moving [13]. In the same vein, there is no reason time cannot be considered in the design of metamaterials. On the contrary, the use of time as a tunable variable may open new vistas and applications not sought before in many fields of applied physics. For instance, recent works [14] have shown the importance of time modulation in obtaining nonreciprocal effects of the so-called luminal metamaterials in the context of electromagnetism. In fact, time started recently to be considered, along with geometry [15], as a design parameter for newly proposed spacetime metamaterials and metasurfaces, with many unprecedented applications [16], such as Fresnel drag [17], signal amplification [18], harmonic generation [19], and photonic circulators [20,21], to name a few. Some earlier studies considered dispersion

relations in spacetime periodic media [22,23] and the dynamics of light propagation in these structures [24,25]. Interestingly, similar effects have been observed in the context of acoustic and mechanical waves in time-modulated structures [26,27].

On the other hand, flexural-gravity waves obey a sixth-order partial differential equation (PDE) and describe the flexural motion [28,29] in thin elastic plates floating atop inviscid and incompressible fluids (e.g., water) [30]. For instance, man-made engineered offshore structures, such as airports or newly built floating islands [31,32], are considered as thin-mat configurations where the horizontal dimensions extend for a few kilometers and the thickness is around a few meters. Moreover, these structures are usually located in the offshore zone, where the depth of water is small, i.e., in the range of 20 m (shallow-water approximation). Furthermore, both the wavelength and the lateral dimensions of the plates (elastic structures) are much larger than its thickness  $\delta$  (see Fig. 1), so one can safely assume the thin-plate (biharmonic) approximation [33–35] or the Kirchhoff-Love plate theory [28]. Characterizing the scattering from such waves by buoyant objects is an active topic of research [36–39] with many applications, such as a dispersionless weakly nonlinear flexural-gravity wave packet [40] or invisibility cloaking for such waves using both transformation optics [41] and the scattering cancellation technique, which was shown to possess intriguing properties from simple cylindrical thin plates [42].

In this paper, we consider time modulation as well as spacetime modulation in the realm of this peculiar type of waves, which are intrinsically different from acoustics and electromagnetism, due to the asymmetric role played by the space and time variables (space of order 6 and time of order 2). This asymmetry will be shown to lead to some intriguing properties of the band gap, not seen before for other wave systems. The remainder of this paper is organized as follows: We start by formulating the problem with an adequate

\*mohamed.farhat@kaust.edu.sa

†ying.wu@kaust.edu.sa

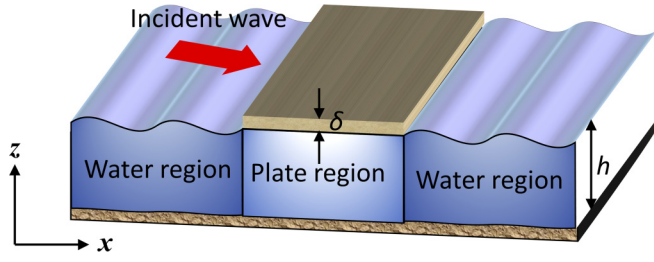


FIG. 1. Schematic of a floating thin plate of thickness  $\delta$  atop shallow seawater of depth  $h$ , in the  $x$ - $z$  plane. The thin plate is supposed to be infinitely extended along the  $y$  direction. The parameters of the plate are as follows: Young's modulus  $E = 50$  GPa, thickness  $\delta = 10$  m, Poisson's ratio  $\nu = 0.34$ , and density of  $900$  kg/m<sup>3</sup>, to make it float atop water.

governing equation and boundary conditions. Then, we focus on investigating the time modulation of flexural-gravity waves by imposing either a time-varying flexural rigidity or a spacetime modulation using an analytical model that results in closed-form expressions by coupling two modes, to gain insight into the underlying physical mechanisms. Next, we solve numerically the full problem by coupling a higher number of modes and verifying the numerical convergence of the results. The results feature a peculiar behavior of the  $k$ -band gap. We discuss also the origin of this effect such as the non-Hermiticity of the system by the spacetime modulation and the appearance of exceptional points (EPs) at the edges of the band gap as well as nonreciprocal wave propagation. We also investigate the sensitivity of the EP on external parameters and fit it analytically using the Puiseux series. Finally, we summarize the obtained results and provide some derivations and further discussion in Appendixes A–C.

## II. PROBLEM SETUP

Flexural-gravity waves obey in the case of the approximations described above and for harmonic variation (in the frequency domain) (see Appendix A) the sixth-order PDE, i.e.,

$$D\Delta^3 W + \rho g \Delta W + \frac{\rho}{h} \omega^2 W = 0, \quad (1)$$

in terms of the water elevation (or plate vertical displacement in the plate's region) [or similarly in terms of the velocity potential  $\varphi$ , related to  $W$  through  $\partial_t W = -h\Delta\varphi$ , as seen in Eq. (A7)] and angular frequency of the water waves  $\omega$ , with  $\rho = 10^3$  kg/m<sup>3</sup> and  $h = 20$  m being the density and depth of water, respectively,  $g = 9.81$  m/s<sup>2</sup> being the acceleration due to terrestrial gravity, and  $D = E\delta^3/[12(1 - \nu^2)]$  being the flexural rigidity of the plate (see Appendix A for a detailed derivation of this PDE and justification of the approximations used). The first term of Eq. (1) stands for the flexural effect (flexural rigidity is driving the surface elevation and thus the velocity potential), while the second term accounts for surface gravity effects (waves, as suggested by the presence of the Laplacian operator  $\Delta$  and surface gravity  $g$ ) [43].

Moreover, the dispersion relation of this kind of waves is obtained by replacing  $\Delta$  by  $(i\beta_1)^2$ , with  $\beta_1$  being the flexural-gravity wave number, i.e.,  $\omega^2 = (hD/\rho)\beta_1^6 + g h \beta_1^2$ .

The interplay between surface gravity waves and flexural waves is evidenced by the presence of both the classical flexural-gravity wave number  $\beta_1^6 = \rho\omega^2/(hD)$  and the surface gravity wave number  $k_0 = \omega/\sqrt{gh}$ . Due to the coupling between flexural and water waves, the analysis of such a system including the derivation of the transfer matrix requires some specific treatment [44].

## III. MODULATION FOR FLEXURAL-GRAVITY WAVES

### A. Time modulation for flexural-gravity waves

Let us consider time modulation of a floating thin plate. This is the analog of time modulation of the permittivity in photonic crystals [45] by allowing a periodic evolution of the flexural rigidity, i.e.,  $D(t + T) = D(t)$ , with a temporal period  $T$ . Regarding a possible experiment, in order to change the elastic parameters directly, one can add shunted external circuits, with tunable electrical properties (resistance, capacitance, and inductance) {see the Supplemental Material (SM) [43] for more details on the piezoelectric potential modeling [46–52]}. Equation (1) shall be rewritten in the time domain and in the one-dimensional (1D) scenario

$$\gamma(t) \frac{\partial^6 W(x, t)}{\partial x^6} + \gamma_1 \frac{\partial^2 W(x, t)}{\partial x^2} - \frac{\partial^2 W(x, t)}{\partial t^2} = 0, \quad (2)$$

with  $\gamma(t) = hD(t)/\rho$  and  $\gamma_1 = gh$ , by assuming that  $\rho$  and  $h$  are time independent. The modulated parameter can be expressed as  $\gamma(t) = \gamma_0[1 + \delta_m \cos(\Omega_m t)]$ , with  $\delta_m = \gamma_m/\gamma_0$  and  $\gamma_0 = hD_0/\rho$  being the nonmodulated parameter. Using the Bloch theorem, applied to the time periodicity [53], we can express the water elevation as

$$W(x, t) = e^{-i(\omega t - \beta_1 x)} \sum_{n=-\infty}^{\infty} \widehat{W}_n e^{-in\Omega_m t}. \quad (3)$$

By inserting Eq. (3) into Eq. (2) and by assuming  $\delta_m = 0$ , we can get the dispersion of plane waves in free space, shown in Fig. 2(a). The free-space eigenmodes can be thus obtained by finding the zeros of the determinant of the diagonal matrix  $\text{diag}[\gamma_0\beta_1^6 + \gamma_1\beta_1^2 - (\omega + n\Omega_m)^2]$ . From this dispersion, its high-order polynomial nature, which is completely different from that of the acoustics or electromagnetism linear behavior, can be clearly seen. This peculiarity is more apparent for low wave numbers, when the dispersion is nearly flat.

In Fig. 2(a), we plot the dispersion at low frequency using two different PDEs [one using Eq. (1) and the other one omitting the second Laplacian operator]. Although the two methods give similar results, the inset clearly displays certain discrepancies and demonstrates the need for using the PDE of Eq. (1). The interesting effects due to time modulation take place when  $\delta_m \neq 0$ . Solving Eq. (2) by using a Fourier expansion of  $W(x, t)$  when  $\delta_m \neq 0$  is generally not possible analytically, as one has to consider an infinite number of terms in the expansion, for finite coupling. So, numerically this expansion is truncated and convergence is verified, in order to obtain the dispersion diagrams. Yet, the coupling between two bands (modes) is insightful and captures the essence of the phenomena (as for the harmonic oscillator or the two-level system in quantum physics [54]). We consider the bands  $n = 0$  and  $n = -1$  [i.e.,  $\widehat{W}_0$  and  $\widehat{W}_{-1}$ ; see Eq. (3)].

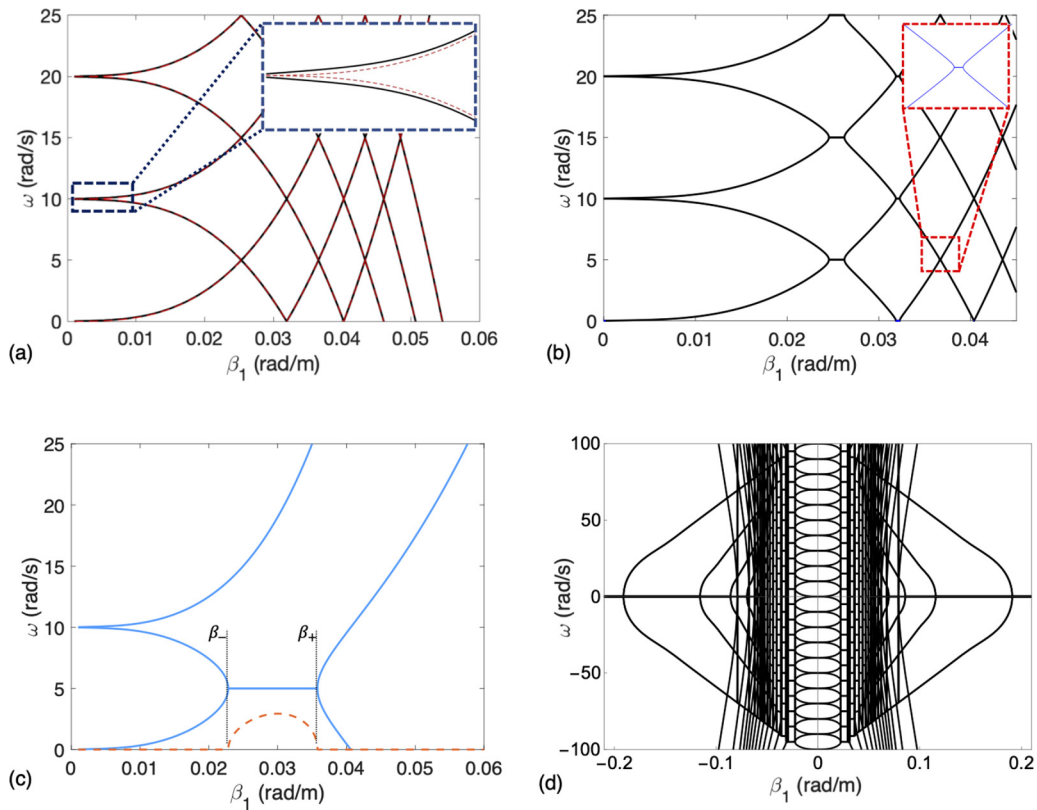


FIG. 2. (a) Dispersion curves of free plane waves (i.e.,  $\delta_m = 0$ ) in floating thin plates for  $N = 5$  (i.e., considering 11 bands) and for  $\Omega_m = 10$  rad/s. The inset shows an enlarged view at low frequency using two different PDEs (see Appendix A). (b) Dispersion curves for  $\delta_m = 0.4$ , where the inset shows the  $k$ -band gap around the angular frequency  $\omega = \Omega_m/2$ . The number of bands and modulation frequency are the same as in (a). The inset shows a magnified view around the second  $k$ -band gap. (c) Two-band dispersion curves for the case of  $\delta_m = 1.75$ , i.e., considering only the bands  $n = 0$  and  $n = -1$ . The width of the  $k$ -band gap ( $[\beta_-, \beta_+]$ ) can be calculated analytically in this case. (d) Broader domain for the dispersion similar to (b), i.e., with  $\Omega_m = 10$  rad/s, but for  $\delta_m = 1.9$  and considering  $N = 10$ , i.e., 21 bands.

The characteristic equation of this coupled system is

$$\begin{vmatrix} \gamma_0 \beta_1^6 + \gamma_1 \beta_1^2 - \omega^2 & \frac{\gamma_0 \delta_m}{2} \beta_1^6 \\ \frac{\gamma_0 \delta_m}{2} \beta_1^6 & \gamma_0 \beta_1^6 + \gamma_1 \beta_1^2 - (\omega - \Omega_m)^2 \end{vmatrix} = 0. \quad (4)$$

The solution of this characteristic equation gives the four eigenfrequencies, owing to the fourth power of  $\omega$  in Eq. (4) i.e.,

$$\omega_j = \frac{1}{2} (\Omega_m \pm \sqrt{\Omega_m^2 + 4(\gamma_0 \beta_1^6 + \gamma_1 \beta_1^2)} \pm \sqrt{\Omega_m^2 (\gamma_0 \beta_1^6 + \gamma_1 \beta_1^2) + \gamma_0 \delta_m / 2 \beta_1^6}), \quad (5)$$

with  $j = 1 \dots 4$ . Figure 2(c) shows the corresponding curves (real and imaginary parts) versus the flexural-gravity wave number  $\beta_1$ . Interestingly, for  $\omega = \Omega_m/2$  one can notice the emergence of a  $k$ -band gap, i.e., a band gap in the wave-number axis with analogy to the  $\omega$ -band gap when space modulation is enforced, shown in Fig. 3(a). Figure 2(c) is obtained for  $\delta_m = 1.75$ . The emergence of this band gap (real part of  $\omega$ ) is confirmed by the finite imaginary part of  $\omega$  [red curve in Fig. 2(c)], which shows that no propagation can take place in the interval denoted  $[\beta_-, \beta_+]$ . The limits of this interval in the  $k$  space are

$$\beta_{\pm} = \left( \frac{\Omega_m^2}{2\gamma_0(2 \mp \delta_m)} \right)^{1/6}. \quad (6)$$

Hence, when  $\delta_m \geq 2$ , only one solution is positive, i.e.,  $\beta_-$ , and the band gap becomes of infinite extent, i.e., for  $\beta_1 > \beta_-$  (see the SM for more details [43]). Next, to gain more insight, we need to consider more bands to compute the correct dispersion curves. By inserting the Fourier expansion of the water elevation field in Eq. (2), we get  $\forall n \in \mathbb{Z}$ ,

$$\begin{aligned} & [\gamma_0 \beta_1^6 + \gamma_1 \beta_1^2 - (\omega + n\Omega_m)^2] \widehat{W}_n \\ & + \frac{\gamma_0 \delta_m}{2} \beta_1^6 (\widehat{W}_{n-1} + \widehat{W}_{n+1}) = 0. \end{aligned} \quad (7)$$

In Fig. 2(b) we consider  $\delta_m = 0.4$  and  $\Omega_m = 10$  rad/s, as well as  $N = 5$  (i.e., 11 bands). At frequencies  $(n + 1/2)\Omega_m$ ,  $k$ -band gaps can be observed at different  $\beta_1$  intervals, of different width (the inset shows the narrow band gap at higher  $\beta_1$ ).

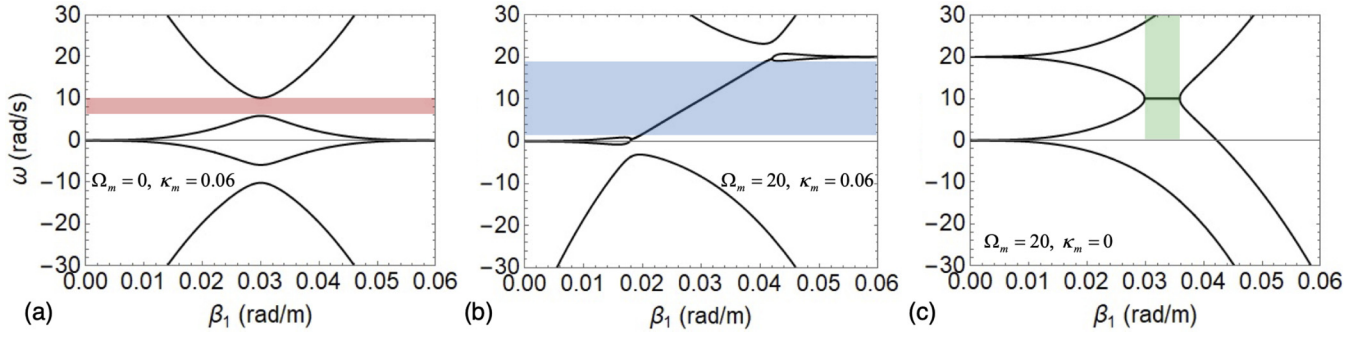


FIG. 3. Two-band dispersion curves for the case of  $\delta_m = 1.75$  and considering only the bands  $n = 0$  and  $n = -1$ , for (a)  $\Omega_m = 0$  rad/s and  $\kappa_m = 0.06$  rad/m, i.e., classical space modulation with frequency band gap, (b)  $\Omega_m = 20$  rad/s and  $\kappa_m = 0.06$  rad/m, i.e., spacetime modulation with an oblique (indirect) band gap, and (c)  $\Omega_m = 20$  rad/s and  $\kappa_m = 0$  rad/m, i.e., classical time modulation with  $k$ -band gap.

Figure 2(d) shows a broader interval of both  $\beta_1$  and  $\omega$ , by taking into account more bands ( $N = 10$ ), demonstrating the peculiarity of time modulation in the framework of flexural-gravity waves. An application of this concept would be filtering and generation of ultranarrowband water-wave signals.

For instance, the picture of the  $k$ -band gap can be seen from another perspective, i.e., that of exceptional points of degeneracy (EPs) [55–57]. The edges of the band gap correspond also to EPs as these are induced by space, time, and/or spacetime modulation. Physically, this is different from gain-loss systems where the EPs are generated due to balanced gain and loss and parity-time ( $PT$ ) symmetry breaking. In fact, Eq. (7) (time modulation) or Eq. (9) (spacetime modulation to be discussed in the next section) can be rearranged in a matrix form by casting the terms with the wave number on the left-hand side, and the problem can be seen as an eigenvalue problem, i.e.,

$$T(\beta_1)\Phi = \omega\Phi, \quad (8)$$

with  $\Phi = [\widehat{W}_{-N}, \dots, \widehat{W}_0, \dots, \widehat{W}_N]^T$  by considering  $2N + 1$  harmonics. The matrix  $T$  is thus  $(2N + 1) \times (2N + 1)$ , and  $\omega$  is the eigenvalue (eigenfrequency) of the modulated system. This means that the results in Fig. 2(c) could be interpreted in a different but equivalent way. Explicitly, at low frequency we have two eigenvalues [both real, i.e., the exact phase of the

system and imaginary part is zero as seen in Fig. 2(c)] that evolve from zero to around  $\beta_1 = 0.023$  rad/m. At  $\beta_1 = \beta_-$ , an EP takes place, and the  $PT$  symmetry is broken, so the system switches to the broken phase. This is demonstrated by the finite imaginary part of the eigenvalue [ $\text{Im}(\omega)$ ] (two complex-conjugate eigenfrequencies). At  $\beta_1 = \beta_+$ , a second EP occurs where the system switches back to the exact phase. For spacetime modulation, the same reasoning can be employed with the only difference that along the broken phase (i.e., interval  $[\beta_-, \beta_+]$ ) the degenerate eigenfrequency is not constant but varies linearly with  $\beta_1$  and results in the oblique band gap as explained in the SM [43]. Further analysis of the sensitivity of the EP is given in Appendix B and shows the effect of various parameters on the EP location as well as the analytical derivation based on the fractional Puiseux series [58,59].

## B. Spacetime modulation and nonreciprocity

### 1. Spacetime modulation

Let us move now to the modulation of the floating plate in spacetime [23], i.e.,  $\gamma(t) = \gamma_0[1 + \delta_m \cos(\kappa_m x - \Omega_m t)]$ , with  $\kappa_m$  being the space-modulation “frequency.” Here, we also consider first the coupling between the bands  $n = 0$  and  $n = -1$ . It is straightforward to show that the dispersion relation is obtained from Eq. (7) by replacing  $\beta_1$  by  $\beta_n = \beta_1 + n\kappa_m$ , i.e.,

$$[\gamma_0(\beta_1 + n\kappa_m)^6 + \gamma_1(\beta_1 + n\kappa_m)^2 - (\omega + n\Omega_m)^2]\widehat{W}_n + \frac{\gamma_0\delta_m}{2}\{[\beta_1 + (n-1)\kappa_m]^6\widehat{W}_{n-1} + [\beta_1 + (n+1)\kappa_m]^6\widehat{W}_{n+1}\} = 0. \quad (9)$$

When only two modes are considered, a characteristic equation similar to Eq. (4) is obtained with the proper changes, i.e.,

$$\begin{vmatrix} \gamma_0\beta_1^6 + \gamma_1\beta_1^2 - \omega^2 & \frac{\gamma_0\delta_m}{2}(\beta_1 - \kappa_m)^6 \\ \frac{\gamma_0\delta_m}{2}\beta_1^6 & \gamma_0(\beta_1 - \kappa_m)^6 + \gamma_1(\beta_1 - \kappa_m)^2 - (\omega - \Omega_m)^2 \end{vmatrix} = 0. \quad (10)$$

In the case of spacetime modulation (or luminal floating structures), the eigenfrequencies are solutions to a sixth-order polynomial, and it is not possible to easily express them in a simple closed form as before. Figure 3(a) shows first the space modulation for comparison, by enforcing  $\Omega_m = 0$  rad/s and  $\kappa_m = 0.06$  rad/m. In this scenario, a classical frequency band gap can be observed and is highlighted in red. Figure 3(b)

gives the plot for  $\Omega_m = 20$  rad/s,  $\kappa_m = 0.06$  rad/m, and  $\delta_m = 0.4$ . Thus, for a finite value of  $\kappa_m\Omega_m$ , we can observe a tilted band gap, towards the  $\beta_1$  axis, i.e., an intermediate state between the  $\omega$ -axis band gap [Fig. 3(a)] and the  $\beta_1$ -axis band gap [Fig. 3(c)]. The regions highlighted in color in Figs. 3(a)–3(c) give the corresponding band gap for each modulation type.

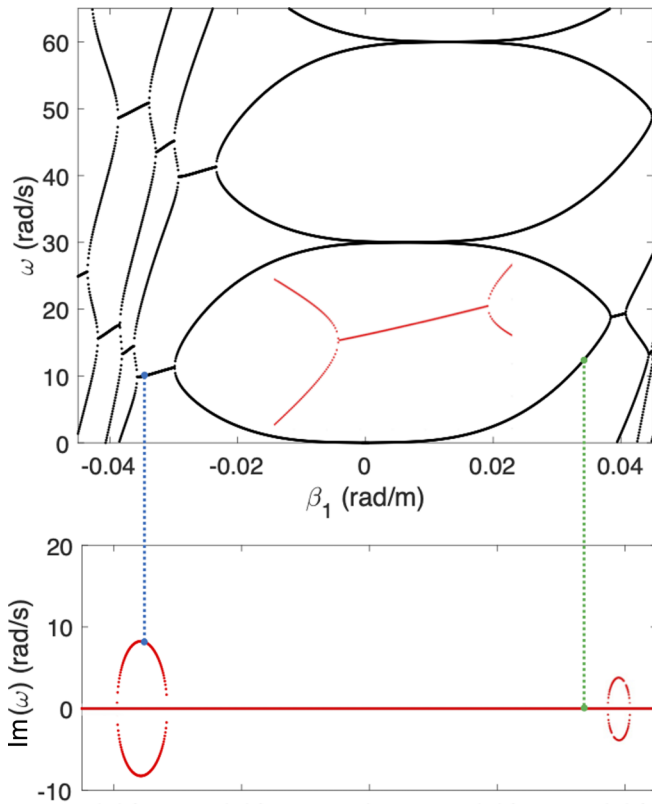


FIG. 4. Top: Dispersion curves for  $N = 5$ , i.e., considering 11 bands for  $\delta_m = 0.8$ ,  $\Omega_m = 30$  rad/s, and  $\kappa_m = 0.0065$  rad/m, where the inset (red curves) is a magnified view of the oblique (rotated)  $k$ -band gap. Bottom: Imaginary part of the first eigenfrequency  $\text{Im}(\omega)$  in the same range of flexural-gravity wave numbers. The blue (green) dots correspond to negative (positive)  $\beta_1 = \mp 0.034$  rad/m.

For the complete treatment, we consider  $N = 5$  (e.g.,  $2N + 1 = 11$  bands) and plot in Fig. 4 the dispersion curves of this luminal floating structure. In comparison with Fig. 2(b), we can see the rotation of the band gap due to the additional space modulation. In the limit where  $\kappa_m/\Omega_m \rightarrow \infty$  we can recover a classical band gap in the frequency domain as demonstrated in Appendix C, Figs. 8 and 9. However, these tilted band gaps are a unique feature of spacetime-modulated thin plates and are due to the fact that in electromagnetic or acoustic systems, time and space have some sort of “duality,” i.e., they can exchange their positions in the equation (up to the speed of the wave) while still getting the same solution. However, in thin plates, time and space are not interchangeable, as exemplified by the governing PDE of Eq. (1) and the corresponding dispersion relation. In the SM, we show an investigation of the role of this asymmetry between space and time in different wave systems [e.g., acoustics (order 2), flexural (order 4), and flexural-gravity (order 6)] as well as hypothetical PDEs. In Fig. S3 of the SM [43], only the acoustic waves (equal order between space and time) do not present an oblique band gap, due to the symmetry between space and time. The other PDEs have different space and time orders and thus possess tilted band gaps, confirming thus the origin of the tilted band gap. The same effect is also seen in Fig. 3(b) for the simple case of coupling between two bands (see Appendix C for the progres-

sion of the band gap with varying space- and time-modulation frequencies, showing a nontrivial dependence).

## 2. Nonreciprocity and unidirectionality

Figure 4 showcases another intriguing property directly originating from spacetime modulation, i.e., nonreciprocity. For instance, to grasp these nonreciprocal features, we plot the eigenfrequencies (or dispersion relation) for a flexural-gravity wave number  $\beta_1$  spanning the range  $[-0.045, 0.045]$  rad/s. Due to the tilting of the band gaps (owing to spacetime modulation) and the overall rotation of the band diagram, we clearly observe a strong asymmetrical behavior for positive and negative opposite values of  $\beta_1$ . For example, the operation point marked with a green dot ( $\beta_1 = 0.034$  rad/s) and the one marked with a blue dot ( $\beta_1 = -0.034$  rad/s and opposite to the green one) have markedly different properties. The blue point lies in a band-gap region where no propagation is possible, while the green point corresponds to the propagating regime (this is confirmed by the observation of the imaginary part of the eigenfrequencies: finite or zero, respectively). Hence our spacetime metamaterial may be used for unidirectional water-wave propagation (only right-direction propagation is possible in this specific case). In a sense, our spacetime modulation plays the role of topologically nontrivial metal-metal interfaces, where these structures were shown to result in unidirectional propagation of plasmons due to the topology of the band structure [60,61]. Here, we propose a unidirectional device for flexural-gravity waves without the use of complex strategies (such as the presence of a magnetic field in plasmonics or the use of gain and loss systems).

On the application side, this idea may open avenues for control and harvesting of water waves in floating thin elastic systems. In fact, cities and critical infrastructure located near coastlines are subject to flooding, and thus floating systems might play a role in the near future by either replacing some of the existing infrastructure (airports and artificial islands) or helping to protect and isolate land from some ocean waves. Our nonreciprocal floating metamaterial can be of use as it will selectively stop water waves that are incoming from a preferred direction.

## IV. CONCLUDING REMARKS

To conclude, flexural-gravity waves are investigated, and their scattering properties are quantified in the context of spacetime modulation of floating plates. In this context, we must handle the coupling between water waves and flexural waves of thin floating plates. It is shown that these waves possess one propagating and two evanescent solutions, responsible for the observed effects. As a potential application, we consider a time modulation of the Young’s modulus both in time and spacetime, and we show the emergence of a  $k$ -band gap with peculiar properties as well as tilted band gaps. This results, in particular, in nonreciprocal features with evident use for unidirectional propagation of flexural-gravity waves. The presented research may open vistas in manipulation and harvesting of water waves in floating structures, with promising applications in maritime engineering.

For instance, one intriguing application may be the rainbow trapping of water waves by leveraging of spacetime modulation in order to collect some of the ocean energy and then convert it to useful electricity via piezoelectric materials, for example. Thus it can be clearly seen that spacetime modulation in the realm of floating thin plates can have a plethora of intriguing applications and novel properties not found with other classical waves (i.e., obeying the Helmholtz equation).

Regarding the issue of practical realization, if the goal is to model and design spacetime metamaterials for floating megastructures such as floating airports or artificial islands, megastructures of sizes ranging from a few hundreds of meters to kilometers have to be studied. Of course, this is a long-term experiment that requires great accuracy in the modeling. For instance, to model such megastructures, one cannot consider a fixed height (or depth of water). Also, the thickness of the plate and its material elastic properties (Young's modulus and Poisson's ratio) may vary from one region to another depending on the structure and the application being tackled. Thus a more detailed numerical modeling needs to be developed and performed, for example, by using finite-element methods devoted to fluid dynamics that would account for various nonlinear effects beyond the scope of our study. Yet, it should be emphasized that our concept is scalable and that it can work efficiently for a much smaller scale that may be used, for example, in other applications such as energy harvesting (see the SM for some results [43]).

## ACKNOWLEDGMENTS

The research reported in this paper was supported by King Abdullah University of Science and Technology (KAUST) Office of Sponsored Research (OSR) under Grants No. OSR-2016-CRG5-2950 and No. OSR-2020-CRG9-4374, as well as KAUST Baseline Research Fund BAS/1/1626-01-01. P.-Y.C. would like to acknowledge KAUST Grant No. CRG-4056.2 for supporting the research reported in this paper. The authors would also like to acknowledge useful comments by anonymous referees that helped in improving the quality of this work.

## APPENDIX A: FLEXURAL-GRAVITY GOVERNING EQUATION

### 1. Derivation

The structures considered in this paper are thin elastic plates floating atop water. The thickness  $\delta$  of a given plate is assumed to be very small in comparison to its lateral dimensions  $L_p$  and the wavelength of the water waves, i.e.,  $0 < \delta \ll L$  and  $0 < \delta \ll \lambda$ . Also, we assume that the depth of water  $h$  is small in comparison to the wavelength, i.e., the shallow-water approximation, which is  $0 < h \ll \lambda$ . Furthermore, it is assumed that the flow of water is irrotational; thus the velocity field can be expressed as  $\mathbf{v} = \nabla\varphi$ , with  $\varphi$  being the velocity potential. The water elevation in the plate's region is denoted as  $W$ . Thanks to the shallow-water equation, one has

$$\frac{\partial W}{\partial t} + h\Delta\varphi = 0. \quad (\text{A1})$$

In the plate's region, one can express the relationship between the liquid elevation and pressure exerted by the thin plate using the linearized Bernoulli equation, i.e.,

$$p = -\rho gW - \rho \frac{\partial \varphi}{\partial t}, \quad (\text{A2})$$

where  $g = 9.81 \text{ m/s}^2$  is the surface gravity of the Earth and  $\rho$  is the mass density of water. Last, the pressure exerted by the plate can also be expressed by the dynamic condition as

$$p = D\Delta^2 W + M \frac{\partial^2 W}{\partial t^2}, \quad (\text{A3})$$

where the Laplacian  $\Delta$  is understood as operating in the two-dimensional space, i.e., in the  $x$ - $y$  plane. Moreover,  $M$  is the surface density of the plate (i.e., unit of mass per unit of surface), and  $D$  is its flexural rigidity. By combining Eqs. (A1)–(A3) and taking the time derivative of both Eqs. (A2) and (A3), one can derive the equation obeyed by the velocity potential in its domain of validity, in the case of isotropic and homogeneous physical parameters, i.e.,  $D$ ,  $h$ ,  $M$ , and  $\rho$ , which is

$$D\Delta^3\varphi + M \frac{\partial^2}{\partial t^2}\Delta\varphi + \rho g\Delta\varphi - \frac{\rho}{h} \frac{\partial^2\varphi}{\partial t^2} = 0. \quad (\text{A4})$$

Yet, in the case in which the flexural rigidity  $D$  depends on time, it is more convenient to write the PDE in terms of  $W$  by taking the Laplacian of Eqs. (A1)–(A3). This leads to

$$D\Delta^3 W + M \frac{\partial^2}{\partial t^2}\Delta W + \rho g\Delta W - \frac{\rho}{h} \frac{\partial^2 W}{\partial t^2} = 0. \quad (\text{A5})$$

### 2. Approximations

Let us denote the terms of Eq. (A4) by

$$T_1 = D\Delta^3\varphi, \quad T_2 = M\partial_t^2\Delta\varphi,$$

$$\text{and } T_3 = \rho g\Delta\varphi \approx \rho/h\partial_t^2\varphi.$$

The second term, i.e.,  $T_2$ , of this equation can be shown to be less significant than the remaining ones, so it can be ignored, as with our set of approximations, this term is much smaller than the remaining terms of the left-hand side of Eq. (A4). Figure 5(a) compares the terms  $T_2$  and  $T_3$  versus the wavelength of water waves. It shows that for most of the spectrum, the term  $T_2$  can be safely ignored. The exception occurs only for small wavelengths. However, since we are working in the shallow-water approximation, we do not consider these wavelengths, and hence  $T_2$  can be neglected. Thus the equation satisfied in the plate's region is

$$D\Delta^3\varphi + \rho g\Delta\varphi - \frac{\rho}{h} \frac{\partial^2\varphi}{\partial t^2} = 0. \quad (\text{A6})$$

In the frequency domain, when we assume a time-harmonic dependence, i.e.,  $\partial/\partial t = -i\omega$ , we obtain (by uniformly and interchangeably denoting the velocity potential and its harmonic component by  $\varphi$ )

$$\Delta^3\varphi + \frac{\rho g}{D}\Delta\varphi + \frac{\rho}{hD}\omega^2\varphi = 0. \quad (\text{A7})$$

Evidently, the same approximations apply to Eq. (A5), i.e.,

$$\Delta^3 W + \frac{\rho g}{D}\Delta W + \frac{\rho}{hD}\omega^2 W = 0. \quad (\text{A8})$$

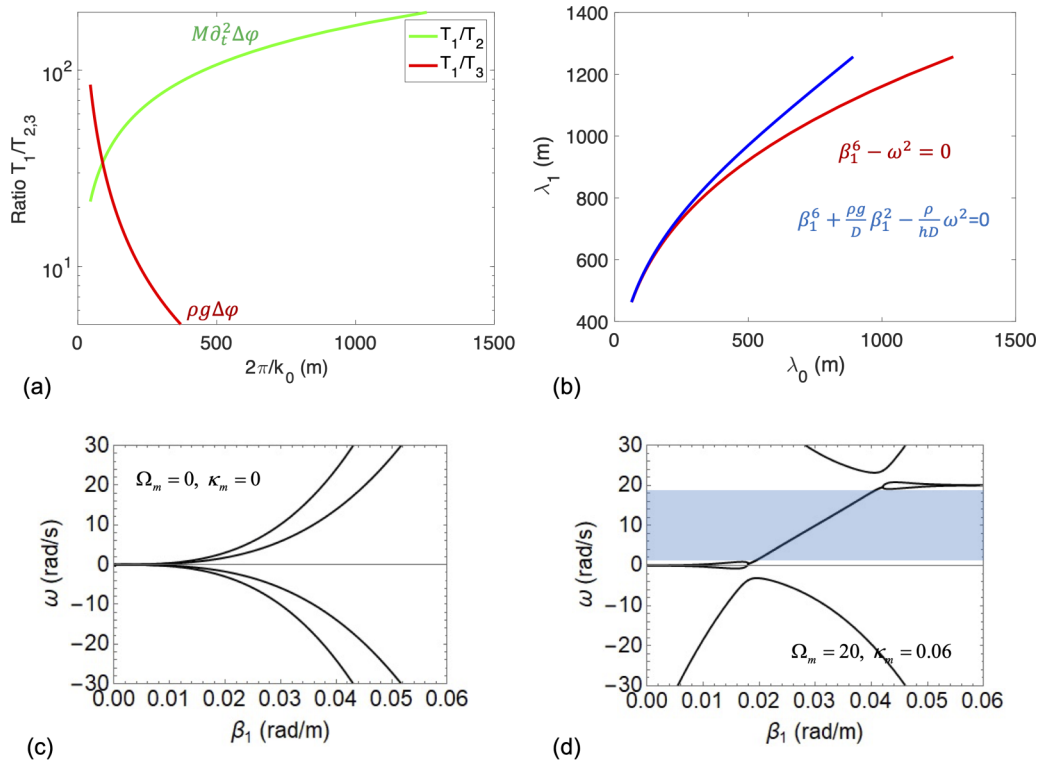


FIG. 5. (a) Comparison of the strength of the terms  $T_2$  and  $T_3$ , using dimensional analysis, normalized by the first term  $T_1$ , vs the water wavelength  $\lambda_0 = 2\pi/k_0$ . (b) Dispersion relation (flexural wavelength vs water wavelength) of flexural-gravity waves, using the PDE of Eq. (A7) and the other PDE [same as in Eq. (A7) without the term  $T_2$ ]. (c) Two-band dispersion curves in free space, i.e., no coupling,  $\delta_m = 0$ . (d) Two-band dispersion considering only the bands  $n = 0$  and  $n = -1$ , for  $\Omega_m = 20$  rad/s,  $\kappa_m = 0.06$  rad/m [spacetime modulation with an oblique (indirect) band gap], and  $\delta_m = 1.75$ .

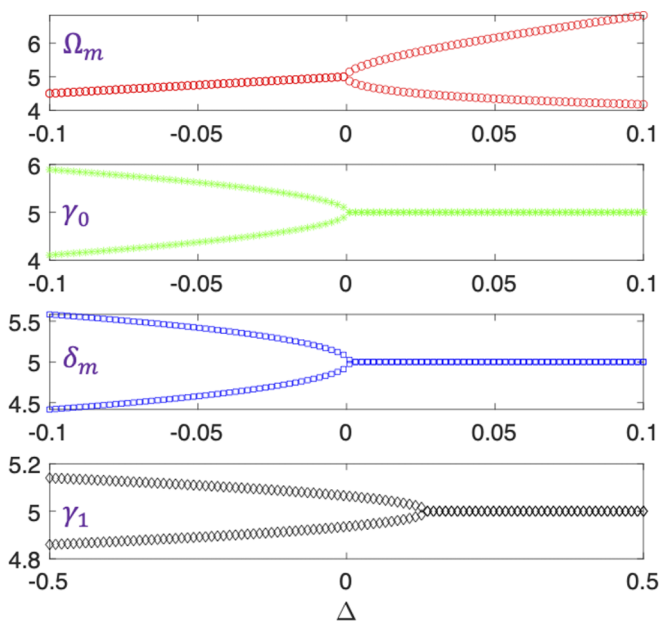


FIG. 6. Variation of the eigenfrequencies  $\omega$  vs the normalized perturbation parameter  $\Delta$  computed numerically for  $\Lambda = \Omega_m$ ,  $\Lambda = \gamma_0$ ,  $\Lambda = \delta_m$ , and  $\Lambda = \gamma_1$  reading from top to bottom, respectively. The parameters of the spacetime modulation are  $\Omega_m = 10$  rad/s and  $\delta_m = 1.75$ , while the other parameters are the same as in the main text.

Figure 5(b) plots the dispersion relation of Eq. (A7) and that of the other PDE, where the term  $T_3 = \rho g \Delta$  is neglected. The two PDEs coincide at small wavelengths, but as the wavelength increases, the mismatch increases considerably.

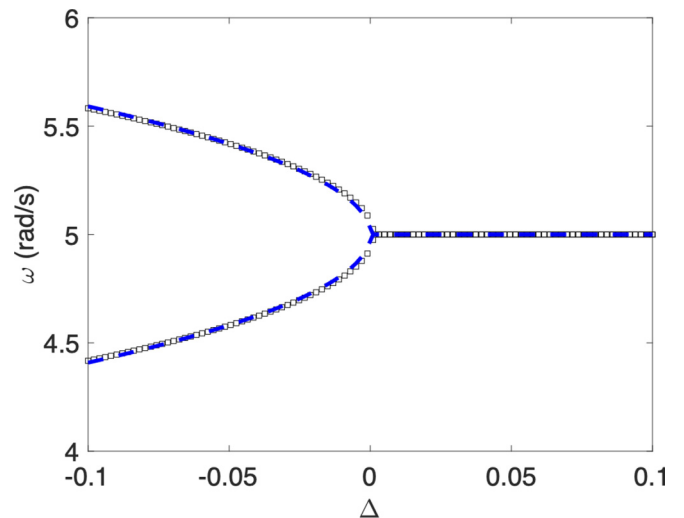


FIG. 7. Analytical (blue dashed line) and numerical (black squares) calculation of the variation of the eigenvalues vs the normalized perturbation parameter  $\Delta$ , with the remaining properties being the same as in Fig. 6.

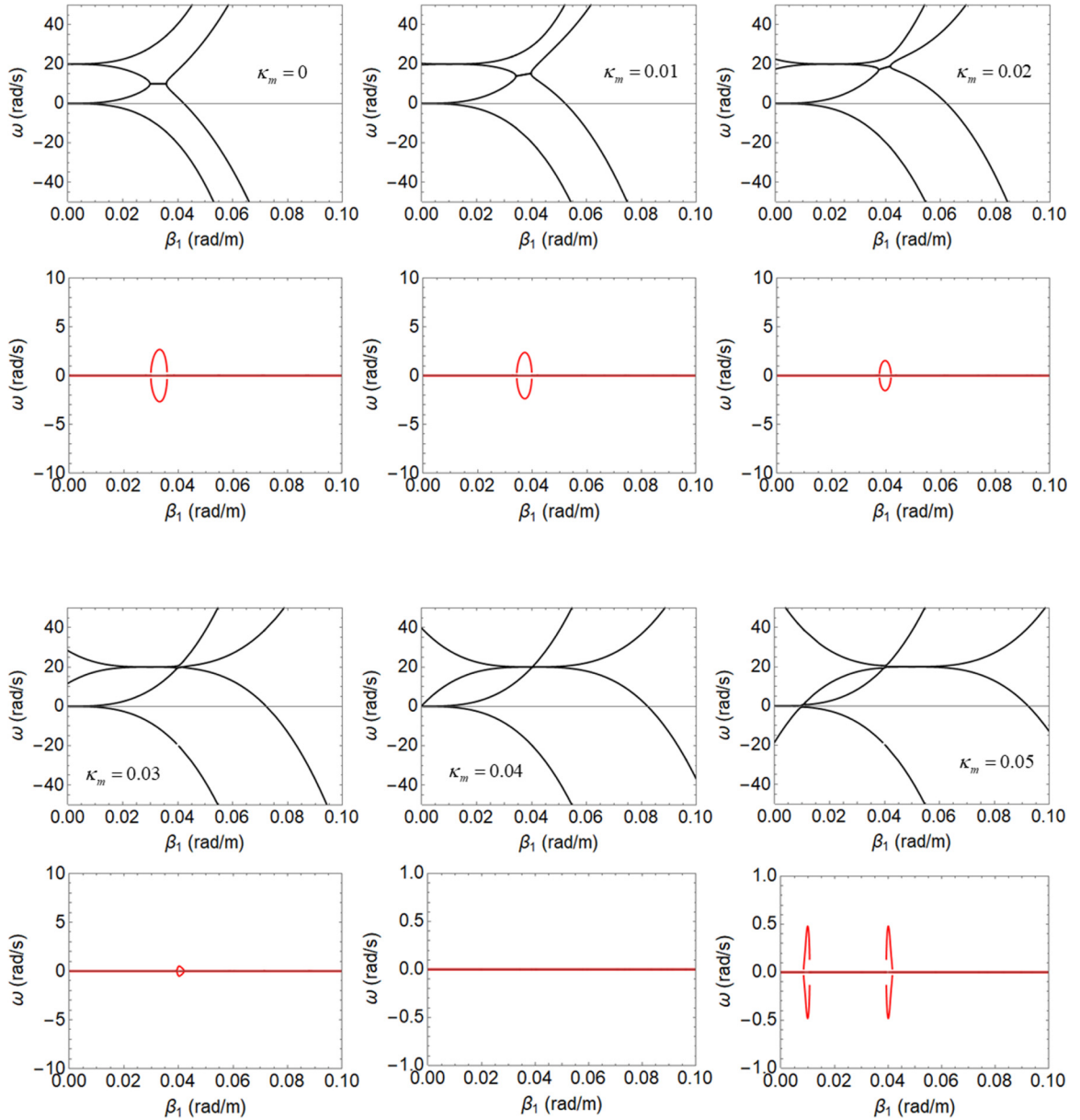


FIG. 8. Two-band dispersion curves for the case of  $\delta_m = 1$  and considering only the bands  $n = 0$  and  $n = -1$ , for  $\Omega_m = 20$  rad/s and for varying  $\kappa_m$  from 0 to 0.05 rad/m (spacetime modulation with an oblique, i.e., indirect, band gap). The black curves show the real part of the eigenfrequencies, while the red curves show their imaginary part. The remaining physical parameters of the elastic plate and liquid are the same as those defined in Sec. II of the main text.

### 3. Boundary conditions

In order to solve a scattering problem involving Eqs. (A7) or (A8), we need to supply the boundary conditions, which in the case of a plate-plate boundary, consists in ensuring the continuity of the six parameters  $\partial_t \varphi$ ,  $\partial_n \varphi$ ,  $\Delta \varphi$ ,  $\partial_n(\Delta \varphi)$ ,  $M_n(\Delta \varphi)$ , and  $V_n(\Delta \varphi)$ , corresponding to the six unknowns (see Fig. 1 of Ref. [32]), with  $n$  being the normal to the boundary and  $s$  being the tangential coordinate, i.e.,

$$M_n(\Delta \varphi) = -D \left( \frac{\partial^2 \Delta \varphi}{\partial n^2} + \nu \frac{\partial^2 \Delta \varphi}{\partial s^2} \right),$$

$$V_n(\Delta \varphi) = \frac{\partial M_n(\Delta \varphi)}{\partial n} - 2 \frac{\partial M_{ns}(\Delta \varphi)}{\partial s},$$

where the operator  $M_{ns} = D(1 - \nu)\partial^2/\partial n \partial s$  and where  $\partial_t$ ,  $\partial_n$ , and  $\partial_s$  denote the partial derivative with respect to time, the normal component, and the tangent component, respectively. For a plate-water boundary, we have instead four boundary conditions, which are continuity of  $\partial_t \varphi$  as well as  $\partial_n \varphi$  and  $M_n = V_n = 0$  [32]. In the case of a layered structure such as the one shown in Fig. 1 of the main text, these conditions simplify greatly as can be shown easily.

### 4. Evanescent waves

We wish to emphasize here that flexural-gravity waves propagating within a floating thin plate are shown to obey the sixth-order PDE [Eq. (1) of the main text] in the frequency

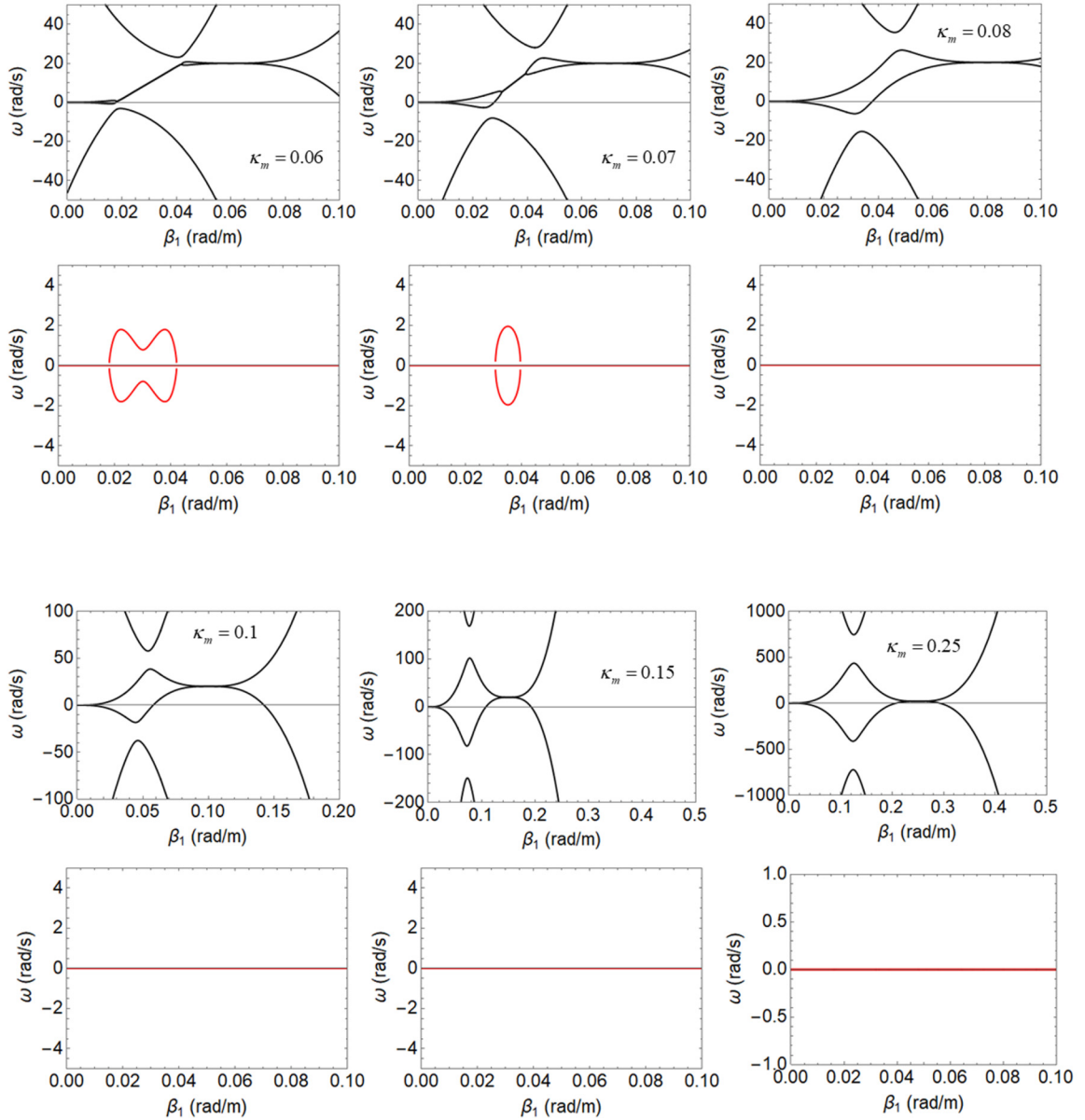


FIG. 9. Two-band dispersion curves for the case of  $\delta_m = 1$  and considering only the bands  $n = 0$  and  $n = -1$ , for  $\Omega_m = 20$  rad/s and for varying  $\kappa_m$  from 0.06 to 0.25 rad/m [spacetime modulation with an oblique (indirect) band gap]. The black curves show the real parts of the eigenfrequencies, while the red curves show their imaginary parts. The remaining physical parameters of the elastic plate and liquid are the same as those defined in Sec. II of the main text.

domain; in addition to propagating flexural-gravity waves, i.e.,  $e^{\pm i\beta_1 x}$ , there exist evanescent (inhomogeneous) flexural-gravity-wave solutions, differentiating the floating plate from its acoustic counterpart (see the SM [43]), in which only propagating waves are considered. In the free propagating domain, only the propagating component survives; as the evanescent wave is proportional to  $e^{\pm\beta_1 x}$  and since these evanescent waves decay exponentially as they travel away from their corresponding interfaces, they do not contribute to the scattering coefficients, which are measured in the far field. However, importantly, in order to fully characterize the scattering of flexural-gravity waves, we have to take into account the contribution of all waves at the inner interfaces of the metamaterial. This is exactly what we do in our treatment,

where these waves (coupled to the other propagating ones) implicitly influence the physics of the spacetime modulation. Hence it should be understood that these waves are present at all steps of the calculation on an equal footing with the propagating ones; in a sense, we solve the full problem without approximation.

#### APPENDIX B: SENSITIVITY OF THE EP AND ANALYTICAL MODELING VIA PUISEUX FRACTIONAL POWER SERIES

The solution of Eq. (8) shows that our problem can be thought of as an eigenvalue problem and that the  $k$ -band gap is reminiscent of EP and parity-time symmetry breaking as dis-

cussed in Sec. III. In the following we analyze the sensitivity of the EP and band gap with respect to small perturbation on the physical parameters of the structure and show the extreme sensitivity of the spacetime-modulation scheme that further demonstrates its inner relation with EPs. Let us consider any parameter that we want to perturb and denote its perturbed value by  $\Lambda_p$  and its value at the EP by  $\Lambda_{EP}$ . Hence the relative perturbation can be given by  $\Delta = (\Lambda_p - \Lambda_{EP})/\Lambda_{EP}$  or equivalently  $\Lambda_p = \Lambda_{EP}(1 + \Delta)$ .  $\Delta$  can thus assume positive or negative values, and in Fig. 6 we plot the effect of this perturbation on the eigenfrequencies for different scenarios, i.e.,  $\Lambda = (\Omega_m, \delta_m, \gamma_0, \gamma_1)$ . We notice that for  $\Lambda = \Omega_m$  the splitting in the eigenfrequencies occurs for  $\Delta > 0$ , whereas for the other scenarios this occurs for  $\Delta < 0$ , showing the peculiar role of perturbing the modulation frequency. Note also that the lower panel corresponding to  $\Lambda = \gamma_1$  has a different scale in the  $x$  axis, as it is two orders of magnitude less sensitive to perturbation than the remaining parameters.

We go one step further and use the Puiseux series, which is a fractional power series used to fit the observed behavior of the eigenfrequencies' variation versus the perturbation  $\Delta$  [58,59,62]. As in our case the eigenvalue is  $\omega$  as given by Eq. (8), it can be shown that the eigenvalues are (here, we have a doubly degenerate EP, so we expect to have two eigenvalues)

$$\omega_{\pm}(\Delta) = \omega_{EP} \pm \tau_1 \sqrt{\Delta}, \quad (\text{B1})$$

where

$$\tau_1 = i \sqrt{\frac{\frac{\partial \mathcal{L}}{\partial \Delta}(\Delta, \omega)}{\frac{1}{2} \frac{\partial^2 \mathcal{L}}{\partial \omega^2}(\Delta, \omega)}}_{\Delta=0, \omega=\omega_{EP}}, \quad (\text{B2})$$

with  $\mathcal{L} = |T(\Delta) - \omega \mathbb{1}|$ , where  $\mathbb{1}$  denotes the identity matrix of the same dimension as  $T$ . The sensitivity of the device is demonstrated by the fact that the eigenfrequencies vary as the square root of the perturbation  $\Delta$ , meaning that a small value

of  $\Delta$  can still result in a dramatic effect on  $\omega_{\pm}$ . Figure 7 plots the comparison between the analytical and numerical calculations of the eigenvalues when  $\Lambda = \delta_m$ , i.e., we perturb the modulation amplitude. In this case, we compute  $\tau_1 = 1.87i$  from Eq. (B2). An excellent agreement is observed for small values of  $\Delta$  demonstrating thus the validity of the analytical method as well as the sensitivity of the spacetime-modulation effect.

### APPENDIX C: TILTED BAND GAP

Here, we wish to understand the origin and variation of the tilted band gap due to spacetime modulation of flexural-gravity waves. Figures 5(c) and 5(d) show the comparison between the two bands in free space and in the case of spacetime modulation, showing how the band gap appears due to coupling.

#### Band-gap variation with modulation

Figures 8 and 9 show the dependence of the oblique (tilted) band gap for a time-modulation frequency  $\Omega_m = 20$  rad/s and for a varying space-modulation frequency  $\kappa_m$  ranging from 0 to 0.25 rad/m. These two figures show how the band gap is gradually transformed from horizontal to vertical, via an oblique band gap of various angles with increasing values of  $\kappa_m$ . These figures show, for instance, a nontrivial behavior (i.e., a nonlinear variation of the band-gap rotation) as the oblique band gap first disappears for  $\kappa_m = 0.03, 0.04$  rad/m and then reappears before transforming into a classical (frequency) band gap when the spatial modulation becomes strong enough (i.e., for  $\kappa_m \geq 0.1$  rad/m). Hence this progression shows that we can get all band-gap types by controlling the spatial-modulation frequency and keeping the time modulation constant or equivalently by sweeping the time modulation for a constant spatial modulation:  $k$ -band gap for  $\kappa_m = 0$  for the first plot in Fig. 8, oblique band gap, and frequency band gap for the remaining plots in Fig. 9.

- 
- [1] W. Cai and V. M. Shalaev, *Optical Metamaterials: Fundamentals and Applications* (Springer, New York, 2010).
  - [2] R. V. Craster and S. Guenneau, *Acoustic Metamaterials: Negative Refraction, Imaging, Lensing and Cloaking*, Springer Series in Materials Science Vol. 166 (Springer, New York, 2012).
  - [3] N. Fang, Z. Liu, T.-J. Yen, and X. Zhang, Regenerating evanescent waves from a silver superlens, *Opt. Express* **11**, 682 (2003).
  - [4] H. Chen, C. T. Chan, and P. Sheng, Transformation optics and metamaterials, *Nat. Mater.* **9**, 387 (2010).
  - [5] M. Kadic, S. Guenneau, S. Enoch, P. A. Huidobro, L. Martin-Moreno, F. J. García-Vidal, J. Renger, and R. Quidant, Transformation plasmonics, *Nanophotonics* **1**, 51 (2012).
  - [6] A. Silva, F. Monticone, G. Castaldi, V. Galdi, A. Alù, and N. Engheta, Performing mathematical operations with metamaterials, *Science* **343**, 160 (2014).
  - [7] B. Assouar, B. Liang, Y. Wu, Y. Li, J.-C. Cheng, and Y. Jing, Acoustic metasurfaces, *Nat. Rev. Mater.* **3**, 460 (2018).
  - [8] J. Mei, Z. Liu, J. Shi, and D. Tian, Theory for elastic wave scattering by a two-dimensional periodical array of cylinders: An ideal approach for band-structure calculations, *Phys. Rev. B* **67**, 245107 (2003).
  - [9] M. Lapine, D. Powell, M. Gorkunov, I. Shadrivov, R. Marqués, and Y. Kivshar, Structural tunability in metamaterials, *Appl. Phys. Lett.* **95**, 084105 (2009).
  - [10] J. Qu, M. Kadic, A. Naber, and M. Wegener, Micro-structured two-component 3D metamaterials with negative thermal-expansion coefficient from positive constituents, *Sci. Rep.* **7**, 40643 (2017).
  - [11] H. Honarvar and M. I. Hussein, Two orders of magnitude reduction in silicon membrane thermal conductivity by resonance hybridizations, *Phys. Rev. B* **97**, 195413 (2018).
  - [12] I. Newton, *Philosophiae Naturalis Principia Mathematica* (G. Brookman, Glasgow, 1833), Vol. 1.

- [13] A. Einstein, Zur Elektrodynamik bewegter Körper, *Ann. Phys. (Berlin)* **322**, 891 (1905).
- [14] E. Galiffi, P. Huidobro, and J. Pendry, Broadband Nonreciprocal Amplification in Luminal Metamaterials, *Phys. Rev. Lett.* **123**, 206101 (2019).
- [15] C. Caloz and Z.-L. Deck-Léger, Spacetime metamaterials, Part I: General concepts, *IEEE Trans. Antennas Propag.* **68**, 1569 (2020).
- [16] C. Caloz and Z.-L. Deck-Léger, Spacetime metamaterials, Part II: Theory and applications, *IEEE Trans. Antennas Propag.* **68**, 1583 (2020).
- [17] P. A. Huidobro, E. Galiffi, S. Guenneau, R. V. Craster, and J. Pendry, Fresnel drag in space-time-modulated metamaterials, *Proc. Natl. Acad. Sci. U. S. A.* **116**, 24943 (2019).
- [18] T. T. Koutserimpas, A. Alù, and R. Fleury, Parametric amplification and bidirectional invisibility in  $\mathcal{PT}$ -symmetric time-Floquet systems, *Phys. Rev. A* **97**, 013839 (2018).
- [19] V. Giniis, P. Tassin, T. Koschny, and C. M. Soukoulis, Tunable terahertz frequency comb generation using time-dependent graphene sheets, *Phys. Rev. B* **91**, 161403 (2015).
- [20] Y. Hadad, J. C. Soric, and A. Alù, Breaking temporal symmetries for emission and absorption, *Proc. Natl. Acad. Sci. U. S. A.* **113**, 3471 (2016).
- [21] D. L. Sounas, C. Caloz, and A. Alù, Giant non-reciprocity at the subwavelength scale using angular momentum-biased metamaterials, *Nat. Commun.* **4**, 2407 (2013).
- [22] E. Cassedy and A. Oliner, Dispersion relations in time-space periodic media: Part I—Stable interactions, *Proc. IEEE* **51**, 1342 (1963).
- [23] E. S. Cassedy, Dispersion relations in time-space periodic media: Part II—Unstable interactions, *Proc. IEEE* **55**, 1154 (1967).
- [24] F. Biancalana, A. Amann, A. V. Uskov, and E. P. O’reilly, Dynamics of light propagation in spatiotemporal dielectric structures, *Phys. Rev. E* **75**, 046607 (2007).
- [25] O. Mattei and G. W. Milton, Field patterns: A new type of wave with infinitely degenerate band structure, *EPL (Europhys. Lett.)* **120**, 54003 (2018).
- [26] H. Nassar, X. Xu, A. Norris, and G. Huang, Modulated phononic crystals: Non-reciprocal wave propagation and Willis materials, *J. Mech. Phys. Solids* **101**, 10 (2017).
- [27] H. Nassar, B. Yousefzadeh, R. Fleury, M. Ruzzene, A. Alù, C. Daraio, A. N. Norris, G. Huang, and M. R. Haberman, Nonreciprocity in acoustic and elastic materials, *Nat. Rev. Mater.* **5**, 667 (2020).
- [28] S. P. Timoshenko and S. Woinowsky-Krieger, *Theory of Plates and Shells* (McGraw-Hill, New York, 1959).
- [29] M. Farhat, P.-Y. Chen, S. Guenneau, K. N. Salama, and H. Bağcı, Localized surface plate modes via flexural Mie resonances, *Phys. Rev. B* **95**, 174201 (2017).
- [30] N. Balmforth and R. Craster, Ocean waves and ice sheets, *J. Fluid Mech.* **395**, 89 (1999).
- [31] Y. Namba and M. Ohkusu, Hydroelastic behavior of floating artificial islands in waves, *Int. J. Offshore Polar Eng. ISOPE-99-09-1-039* (1999).
- [32] G. Zilman and T. Miloh, Hydroelastic buoyant circular plate in shallow water: a closed form solution, *Appl. Ocean Res.* **22**, 191 (2000).
- [33] J. Stoker, *Water Waves: The Mathematical Theory with Applications* (Interscience, New York, 1957).
- [34] M. Kashiwagi, A B-spline Galerkin scheme for calculating the hydroelastic response of a very large floating structure in waves, *J. Mar. Sci. Technol.* **3**, 37 (1998).
- [35] Y. Zimmels and A. Boas, Construction of a pile-based offshore airport, *Ocean Eng.* **30**, 127 (2003).
- [36] M. Meylan, An application of scattering frequencies to hydroelasticity, in *Proceedings of the 11th International Offshore and Polar Engineering Conference, Stavanger, Norway* (ISOPE, Cupertino, CA, 2001), Vol. 3, p. 385.
- [37] W.-M. Lee and J.-T. Chen, Scattering of flexural wave in a thin plate with multiple circular holes by using the multipole Trefftz method, *Int. J. Solids Struct.* **47**, 1118 (2010).
- [38] V. Shemelina, Flexural-gravity circumferential and radial oscillations of a plate floating in shallow water, *J. Appl. Mech. Tech. Phys.* **57**, 550 (2016).
- [39] S. Banerjea, P. Maiti, and D. Mondal, Scattering of flexural gravity waves by a two-dimensional thin plate, *J. Appl. Fluid Mech.* **10**, 199 (2017).
- [40] M.-R. Alam, Dromions of flexural-gravity waves, *J. Fluid Mech.* **719**, 1 (2013).
- [41] A. Zareei and R. Alam, Cloaking by a floating thin plate, in *Proceedings of the 31st International Workshop on Water Waves and Floating Bodies, Michigan, USA* (IWWWFB, Seoul, 2016), pp. 197–200.
- [42] M. Farhat, P.-Y. Chen, H. Bağcı, K. N. Salama, A. Alù, and S. Guenneau, Scattering theory and cancellation of gravity-flexural waves of floating plates, *Phys. Rev. B* **101**, 014307 (2020).
- [43] See Supplemental Material at <http://link.aps.org/supplemental/10.1103/PhysRevB.104.014308> for a comparison of different scenarios with spacetime modulation to explain the physical origin of tilted band gaps for high-order PDEs with up to seventh-order partial derivatives in space, as well as some small-scale versions of the plate and the piezoelectric modeling of the time modulation..
- [44] M. Farhat, S. Guenneau, P.-Y. Chen, and Y. Wu, Parity-time symmetry and exceptional points for flexural-gravity waves in buoyant thin-plates, *Crystals* **10**, 1039 (2020).
- [45] J. R. Zurita-Sánchez, P. Halevi, and J. C. Cervantes-Gonzalez, Reflection and transmission of a wave incident on a slab with a time-periodic dielectric function  $\epsilon(t)$ , *Phys. Rev. A* **79**, 053821 (2009).
- [46] J. Vasseur, A.-C. Hladky-Hennion, B. Djafari-Rouhani, F. Duval, B. Dubus, Y. Pennec, and P. A. Deymier, Waveguiding in two-dimensional piezoelectric phononic crystal plates, *J. Appl. Phys. (Melville, NY)* **101**, 114904 (2007).
- [47] A.-C. Hladky-Hennion and J.-N. Decarpigny, Finite element modeling of active periodic structures: Application to 1–3 piezocomposites, *J. Acoust. Soc. Am.* **94**, 621 (1993).
- [48] Z. Hou and B. Assouar, Tunable elastic parity-time symmetric structure based on the shunted piezoelectric materials, *J. Appl. Phys. (Melville, NY)* **123**, 085101 (2018).
- [49] Z. Hou, H. Ni, and B. Assouar,  $\mathcal{PT}$ -Symmetry for Elastic Negative Refraction, *Phys. Rev. Appl.* **10**, 044071 (2018).
- [50] Q. Wu, Y. Chen, and G. Huang, Asymmetric scattering of flexural waves in a parity-time symmetric metamaterial beam, *J. Acoust. Soc. Am.* **146**, 850 (2019).

- [51] Z. Lu and A. N. Norris, Non-reciprocal wave transmission in a bilinear spring-mass system, *J. Vib. Acoust.* **142**, 021006 (2020).
- [52] M. Farhat, P.-Y. Chen, S. Guenneau, and Y. Wu, Self-dual singularity through lasing and antilasing in thin elastic plates, *Phys. Rev. B* **103**, 134101 (2021).
- [53] K. A. Lurie, *An Introduction to the Mathematical Theory of Dynamic Materials*, Advances in Mechanics and Mathematics Vol. 15 (Springer, New York, 2007).
- [54] J. J. Sakurai, *Advanced Quantum Mechanics* (Pearson Education, Uttar Pradesh, India, 1967).
- [55] M. Y. Nada, M. A. Othman, and F. Capolino, Theory of coupled resonator optical waveguides exhibiting high-order exceptional points of degeneracy, *Phys. Rev. B* **96**, 184304 (2017).
- [56] H. Kazemi, M. Y. Nada, T. Mealy, A. F. Abdelshafy, and F. Capolino, Exceptional Points of Degeneracy Induced by Linear Time-Periodic Variation, *Phys. Rev. Appl.* **11**, 014007 (2019).
- [57] S. Longhi, Floquet exceptional points and chirality in non-Hermitian Hamiltonians, *J. Phys. A: Math. Theor.* **50**, 505201 (2017).
- [58] J. Moro, J. V. Burke, and M. L. Overton, On the Lidskii–Vishik–Lyusternik perturbation theory for eigenvalues of matrices with arbitrary Jordan structure, *SIAM J. Matrix Anal. Appl.* **18**, 793 (1997).
- [59] G. W. Hanson, A. B. Yakovlev, M. A. Othman, and F. Capolino, Exceptional points of degeneracy and branch points for coupled transmission lines-linear-algebra and bifurcation theory perspectives, *IEEE Trans. Antennas Propag.* **67**, 1025 (2018).
- [60] K. L. Tsakmakidis, L. Shen, S. A. Schulz, X. Zheng, J. Upham, X. Deng, H. Altug, A. F. Vakakis, and R. W. Boyd, Breaking Lorentz reciprocity to overcome the time-bandwidth limit in physics and engineering, *Science* **356**, 1260 (2017).
- [61] S. Buddhiraju, Y. Shi, A. Song, C. Wojcik, M. Minkov, I. A. Williamson, A. Dutt, and S. Fan, Absence of unidirectionally propagating surface plasmon-polaritons at nonreciprocal metal-dielectric interfaces, *Nat. Commun.* **11**, 674 (2020).
- [62] K. Rouhi, H. Kazemi, A. Figotin, and F. Capolino, Exceptional points of degeneracy directly induced by space–time modulation of a single transmission line, *IEEE Antennas Wireless Propag. Lett.* **19**, 1906 (2020).